Batteries & Supercaps

Research Article
doi.org/10.1002/batt.202200452

Chemistry Europe
European Chemical Societies Publishing

www.batteries-supercaps.org

Consequences of Different Pressures and Electrolytes on the Irreversible Expansion of Lithium Metal Half Cells

Philip Daubinger,[a] Mara Göttlinger,[a] Sarah Hartmann,[a] and Guinevere A. Giffin.*[a, b]

Lithium metal is considered as the 'holy-grail' among anode materials for lithium-ion batteries, but it also has some serious drawbacks such as the formation of dendritic and dead lithium. In this study, the interplay of external pressure and different carbonate- and ether-based electrolytes on the (ir)reversible expansion of lithium metal during cycling against lithium titanate and lithium iron phosphate is studied. In carbonate-based electrolytes without any additives, lithium metal shows tremendous irreversible expansion and significant capacity reduction at elevated current densities due to the formation of mossy and dead lithium. The addition of fluoroethylene carbonate can reduce irreversible expansion and capacity reduction, especially when a high external pressure is applied. When an ether-based electrolyte is used, the irreversible dilation of the lithium metal is suppressed when applying increased external pressures. Overall, increased external pressure appears to reduce the formation of mossy and dead lithium and improve the performance.

Introduction

The demand for higher energy densities in lithium-ion batteries (LIB) leads to the search for materials with high theoretical capacities. Lithium metal is considered the 'holy-grail' of lithium-based batteries, as it has the highest theoretical specific capacity with 3860 $mAh\,g^{-1}$ and the lowest reduction potential of −3.04 V vs. the standard hydrogen electrode of all possible candidates for the negative electrode.[1,2] By replacing the state-of-the-art (SoA) anode material graphite with lithium metal in a LIB with a transition metal cathode, the specific energy could be increased from ~250 $Wh\,kg^{-1}$ up to ~440 $Wh\,kg^{-1}$.[2] However, there are many obstacles for the widespread use of lithium metal as an anode material, such as poor cyclability, high reactivity, volumetric expansion and safety concerns.[3–6] The dissolution (stripping) and deposition (plating) processes during cycling cause the formation of dendrites. New lithium tends to be deposited at the defect sites of the lithium surface due to the altered electric field and the high atomic mobility of lithium.[7–9] This means that lithium deposition does not necessarily occur at the tip of the dendrites, but at the site with the lowest surface energy.[10] Hence, continuous stripping and plating of lithium leads to the formation of a 'mossy-like' lithium layer on top of the bulk lithium. Further cycling promotes the formation of 'dead' lithium. Dead lithium is a metal that is electrically isolated from the substrate or bulk lithium and thus, no longer takes part in the cycling.

The tremendous volume change during cycling (~4.9 µm for every $mAh\,cm^{-2}$)[2] and the related cracking of the solid electrolyte interphase (SEI) result in high surface area lithium and the formation of a fresh metal surface. Severe side reactions occur due to the high reactivity of lithium which consume lithium and electrolyte. Hence, the thickness of the SEI increases, which in combination with the mossy and dead lithium, increases the ion transport resistance in the double layer. Additionally, dendrite growth can cause short circuits between anode and cathode, which poses a risk for thermal runaway.[3,4] One possible way to tackle the issue of the lithium dendrite formation during cycling is to apply an external mechanical force to the cell which also results in increased pressure onto the surface of the lithium metal. Mechanical pressure, which is also known to enhance the performance of SoA LIB,[11–14] may restrict lithium dendrite formation and extend cycle life.[15–18]

The use of carbonate-based electrolytes in combination with lithium metal results in a short cycle life due the poor deposition morphology of lithium in this electrolyte combined with the high chemical reactivity of the carbonate components with Li, particularly at high current rates.[6,19,20] With the use of ether solvents like dimethoxyethane (DME) in combination with salts like lithium bis(fluorosulfonyl)imide (LiFSI), high rate performance can be achieved in symmetrical lithium cells even at high current densities of 10 $mA\,cm^{-2}$.[21]

In this work, the behavior of lithium metal is studied using different external pressures in combination with different carbonate- and ether-based electrolytes. To do this, lithium metal is cycled against the 'zero-strain' electrode lithium titanate (LTO) and lithium iron phosphate (LFP) to minimize the impact of the counter electrode on the total expansion. The volumetric expansion due to the combined effects of the

[a] P. Daubinger, M. Göttlinger, Dr. S. Hartmann, Dr. G. A. Giffin.
Fraunhofer R&D Center Electromobility
Fraunhofer Institute for Silicate Research
Neunerplatz 2, 97082 Wuerzburg, Germany
E-mail: guinevere.giffin@isc.fraunhofer.de
[b] Dr. G. A. Giffin.
Chemical Technology of Materials Synthesis
Faculty of Chemistry and Pharmacy
Julius-Maximilians-University Wuerzburg
Roentgenring 11, 97070 Wuerzburg, Germany

Supporting information for this article is available on the WWW under https://doi.org/10.1002/batt.202200452

Research Article
doi.org/10.1002/batt.202200452
Chemistry Europe
European Chemical Societies Publishing

formation of the SEI, the deposition of mossy and formation of the dead lithium is investigated in an *operando* dilation cell. Additionally, pressure and electrolyte dependent cycling experiments in a laboratory-scale pouch cell system is done to demonstrate the beneficial impact of certain electrolytes and external mechanical pressure on the performance of the cells.

Results and Discussion

Dilation and preselection of the electrodes

In order to find a counter electrode with limited expansion, the dilation behavior of various SoA and next-generation electrodes was investigated (Figures 1 and S1). Table 1 shows the measured capacity, dilation and the areal capacity related dilation during lithiation and delithiation. From the results, it can be seen that the cell configuration with NCM111 vs. LTO undergoes almost no expansion during cycling. This is consistent with the literature, where LTO is known to be a zero-strain material and NCM111 shows little expansion (~1%) during cycling.[22–25] LFP contracts during delithiation and expands during the lithiation. The dilation of ~0.5 μm per mAh cm^{-2} is relatively small compared to the other electrodes (Table 1). Lithium metal has the largest expansion during plating of ~7.9 μm per mAh cm^{-2}. This expansion cannot be explained solely by the theoretical expansion of the metal during plating (~4.9 μm per mAh cm^{-2}, calculated by using Faraday's law, assuming the deposition of a dense, homogeneous lithium layer).[2] Further increases in the thickness are associated with the SEI and with the deposition of less dense, i.e., dendritic or mossy, lithium. The contraction during stripping is ~−5.4 μm per mAh cm^{-2}, which also is larger than theoretically expected, thus implying stripping of mossy lithium. The irreversible dilation is ~2.5 μm per mAh cm^{-2}, as determined from the difference between the two half cycles, and is associated with the SEI growth and the formation of dead lithium. Although this normally would lead to a loss of a capacity in the cell, the lithium excess in the anode is sufficient to compensate this loss.

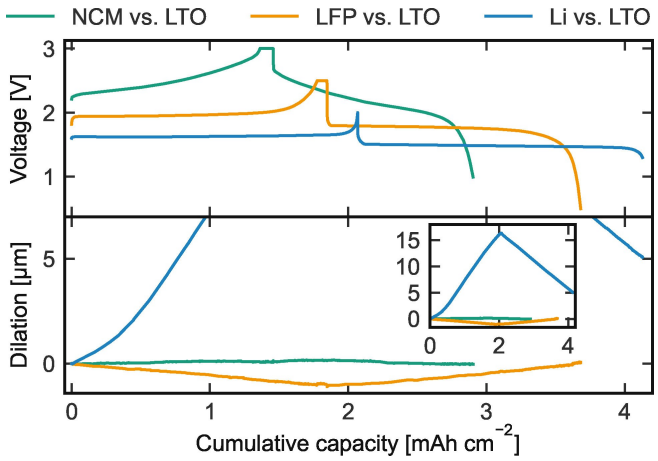

Figure 1. Dilation behavior of NCM111 vs. LTO, LFP vs. LTO and Li vs. LTO during cycling. Voltage and dilation as a function of cumulative capacity. The cells were cycled with Celgard 2500 as separator, LP57 as electrolyte and 0.05 MPa external applied pressure. The current was 2.0 mA cm^{-2} (~1.0 C).

To give a more direct comparison of the expansion of lithium metal to that of other SoA and next-generation electrodes, further configurations were examined (Figure S1). The silicon vs. NCM111 cell has also a significant expansion during lithiation and delithiation (Figure S1 and Table 1). Assuming the negligible cell thickness change of NCM111, the expansion of silicon is ~9 μm which corresponds to a thickness change of ~50% (related to film thickness of the silicon electrode). This is lower than expected based on the theoretically estimated expansion of 280% (on the particle level and assuming full lithiation to $Li_{15}Si_4$).[26,27] Thus, the lower expansion can be related to the high porosity of the electrode (~75%) and the limited utilization of the electrode (~72%). The graphite configurations with LTO or NCM have similar expansion values of 3.2–3.4 μm (~5% expansion, related to film thickness of the graphite electrode). The expansion of the used graphite is lower compared to the theoretical value of ~10% as the capacity is not fully utilized (~78%) and due to the porosity

Table 1. Measured areal capacity, dilation and the dilation per areal related capacity of the investigated cells during lithiation and delithiation of the negative electrode.

	Lithiation			Delithiation			Full cycle
	Areal capacity [mAh cm^{-2}]	Dilation [μm]	Areal capacity related dilation [μm per mAh cm^{-2}]	Areal capacity [mAh cm^{-2}]	Dilation [μm]	Areal capacity related dilation [μm per mAh cm^{-2}]	Irreversible dilation [μm]
NCM111 vs. LTO	1.46	0.10	0.07	1.44	−0.10	−0.07	0
LFP vs. LTO	1.85	−1.00	−0.54	1.83	1.05	0.57	0.05
Lithium vs. LTO	2.07	16.30	7.89	2.06	−11.20	−5.43	5.1
Graphite vs. NCM111	1.74	3.20	1.84	1.72	−3.03	−1.76	0.17
Graphite vs. LTO	1.75	3.44	1.96	1.74	−3.44	−1.98	0
Silicon vs. NCM111	1.83	8.90	4.87	1.74	−8.42	−4.85	0.48

Research Article
doi.org/10.1002/batt.202200452
Chemistry Europe
European Chemical Societies Publishing

of the electrode (~35%). From the results shown in Figures 1 and S1, lithium metal has both the highest reversible and irreversible expansion with 11.2 µm and 5.1 µm, respectively, during cycling at 0.05 MPa external pressure. The irreversible expansion for the other cell configurations is smaller (Table 1). The cells with NCM111, LFP and graphite vs. LTO show negligible irreversible expansion during this cycle. The graphite vs. NCM111 cell shows a small irreversible expansion of 0.17 µm, which can probably be related to some lithium plating on the anode. The silicon vs. NCM111 cell demonstrates a noticeable irreversible expansion of 0.48 µm during one full cycle. This can be explained by the reduced capacity during delithiation of the silicon anode and probably also due to degradation effects, e.g., particle cracking, during the lithiation of the silicon.

To study the impact of the electrolyte and the external applied pressure on the performance and (irreversible) expansion of the lithium metal cells, LTO and LFP were chosen to be the counter electrodes. These two electrodes undergo only a small dilation during cycling and have a good cyclability. Therefore, it may be assumed that LTO and LFP will have only a small impact on the overall expansion of the lithium metal cell. In comparison, NCM111 also has a small dilation, but it is known to be unstable (aluminum corrosion) in contact with the LiFSI-based electrolyte due to its higher potential compared to LFP.[28,29]

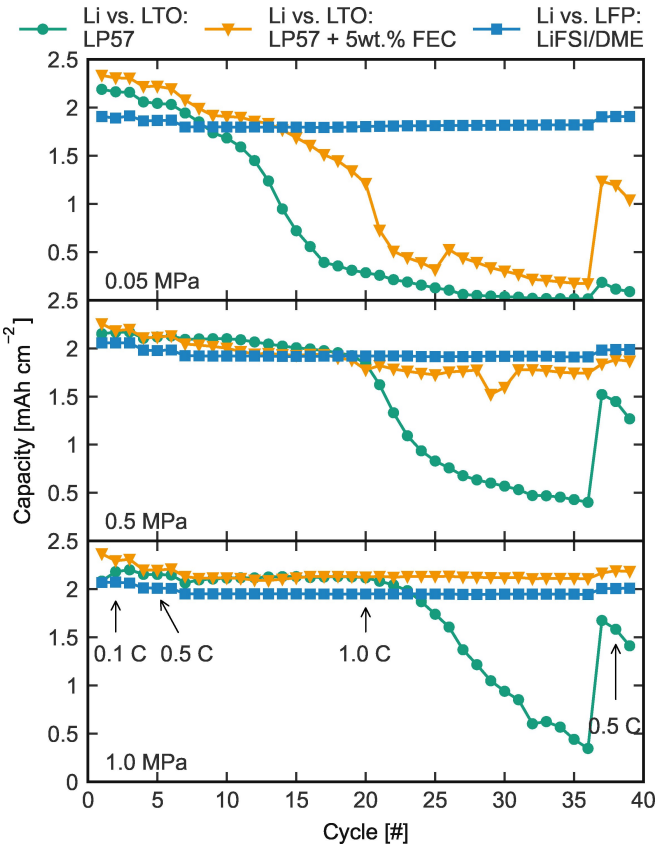

Figure 2. Pressure dependent performance of Li vs. LTO or LFP with three different electrolytes (LP57, LP57 with 5 wt% FEC and 1 M LiFSI in DME). The lines are a guide for the eye only. It should be noted that the LTO electrodes have a slightly higher actual capacity (~2.2 mAh cm^{-2} to ~2.0 mAh cm^{-2}) and hence the discharge capacities are higher compared to the capacities of the LFP electrodes.

Irreversible dilation of lithium metal cells

Figure 2 shows the pressure-dependent discharge capacity of the cells with lithium metal against LTO or LFP and three different electrolytes (i.e., 1 M $LiPF_6$ in ethylene carbonate (EC)/ethyl methyl carbonate (EMC) 3/7 wt% (LP57), LP57 with 5 wt% fluoroethylene carbonate (FEC) and the ether-based 1 M LiFSI in DME) during cycling. The cells with the carbonate-based electrolytes (LP57 and LP57 with 5 wt% FEC) show a different cycling behavior in terms of capacity retention compared to the cells with the ether-based electrolyte. In the initial six cycles (three formation cycles at 0.2 mA cm^{-2}/0.1 C and three 1.0 mA cm^{-2}/0.5 C cycles), the capacity remains constant at ~2.2 mAh cm^{-2} and only a small capacity reduction due to the different current densities is visible. A significant capacity reduction, especially when the low external pressure is applied, is seen for the cells with the carbonate-based electrolytes at higher currents (2.0 mA cm^{-2}/1.0 C). The cells with LP57 (w/o FEC) also show sudden capacity fading at higher pressure, but later in the cycling experiment. For the cells with LP57 w/ 5 wt % FEC, the capacity fading is clearly reduced at elevated pressures, particularly at the highest pressure of 1.0 MPa. When cycling lithium metal with the ether-based electrolyte, no significant capacity reduction is detectable during the cycling experiment regardless of the applied external pressure. This clearly demonstrates a positive impact of both elevated pressure and the replacement of a carbonate-based LP57 electrolyte on the performance of lithium metal half cells. The capacity reduction during cycling is decreased for the cells with LP57 w/ 5 wt% FEC and 1 M LiFSI in DME at elevated pressures, which shows decreased aging phenomena on the lithium metal. A more detailed discussion of the aging phenomena can be found in the following sections.

The dilation of the different cell configurations during cycling is shown in Figure 3. Figures S2–S4 show the dilation of the cells for one 1.0 mA cm^{-2}/0.5 C cycle (Cycle 6). It should be noted that the dilation of the Li vs. LTO cells initially decreases below 0 µm as the LTO electrode gets lithiated at the beginning of the formation. Hence, the lithium ions get stripped from the lithium metal electrode and the total cell thickness decreases. For the Li vs. LFP cells, the LFP electrode is first delithiated in the formation and hence are the lithium ions plated on the lithium metal electrode. In the initial three cycles (0.2 mA cm^{-2}/0.1 C), the reversible dilation is dominant and the irreversible dilation is comparably small. This is also true for the following three cycles (1.0 mA cm^{-2}/0.5 C) for the cells with higher external pressure (0.5 MPa and 1.0 MPa). In contrast, the cells with the lowest pressure have a noticeable irreversible expansion already at this current density. Furthermore, a pressure dependency in the total expansion can be seen. The cells with the lowest external pressure have the highest expansion of ~14–17 µm, while the cells with the highest

Research Article
doi.org/10.1002/batt.202200452
Chemistry Europe
European Chemical Societies Publishing

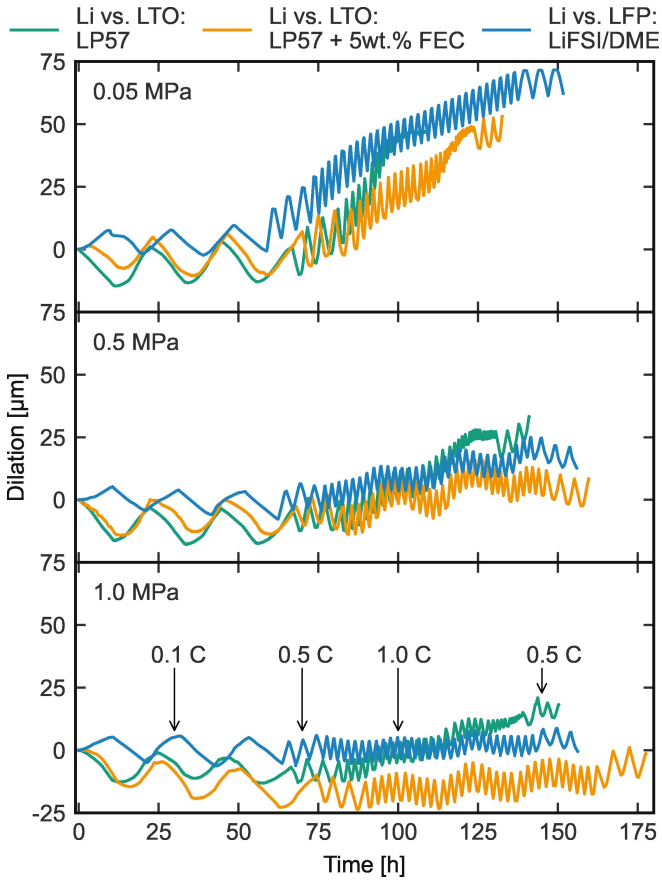

Figure 3. Pressure dependent dilation of Li vs. LTO or LFP with three different electrolytes (LP57, LP57 with 5 wt% FEC and 1 M LiFSI in DME). 1.0 C refers to 2.0 mA cm^{-2}.

pressure show the smallest expansion of ~9–11 µm (Figures S2–S4). This can probably be explained by the reduced formation of mossy and dead lithium at higher pressures. Here, the high pressure probably leads to reduced electrical isolation of the mossy lithium during stripping and hence reduced formation of dead lithium. Furthermore, the high pressure may also reduce the ability of the lithium metal to expand, which may affect the plating morphology.

The cells with LP57 have the most significant irreversible dilation increase at the highest current density of 2.0 mA cm^{-2} at all applied pressures (e.g., 33.2 µm for the pure LP57 cells compared to 8.2 µm for the FEC cells at the end of the test at 0.5 MPa). In contrast, the cells with the FEC additive and ether-based electrolyte only show this behavior at the lowest applied pressure. Interestingly, even though the ether-based cells show a large irreversible expansion at the lowest pressure, the capacity fading is negligible (Figure 2). The reason for this result is not fully understood, but may be related to the morphology and nature of the SEI and needs further investigation. For the higher applied pressures, only a small (0.5 MPa) or negligible (1.0 MPa) irreversible expansion is visible for the cells with FEC additive and ether-based electrolyte. A pressure dependency is evident as the irreversible dilation decreases with increasing external applied pressure for all investigated cells. The cells cycled at the lowest pressure show an irreversible expansion of >47 µm for all electrolytes and only little expansion at the highest pressure, i.e., ~18 µm for the cells with LP57 and ~0 µm for the other cells. The pressure dependency can be mostly related to the reduced formation of mossy and dead lithium at higher pressures due to the better electrical contact of the mossy lithium and the bulk lithium.

Impact of external pressure and electrolyte on the performance

To study the pressure and electrolyte dependent performance of the lithium metal cells for a longer time period, cycling experiments were conducted in laboratory pouch cells with an external bracing device. Figure 4 shows the capacity upon cycling for lithium vs. LTO or LFP. Both systems are cycled with two different electrolytes, the common electrolyte LP57 (both LTO and LFP configurations) and additionally LP57 with 5 wt% FEC and 1 M LiFSI in DME for the lithium vs. LTO system and the lithium vs. LFP system, respectively.

The cells with LP57 show a significant reduction performance in comparison to the cells with both other electrolytes. The lithium vs. LTO cells with LP57 show stable cycling for around 35 cycles, followed by a sudden capacity reduction, which is consistent with the results in the dilation cell (Figure 2). The slope of the capacity drop is pressure dependent, i.e., the cells with no external bracing show the highest slope whereas the cells with the highest pressure have the flattest slope. The threshold of 80% initial capacity is reached by cells without external pressure first, followed by the cells with 0.5 MPa and last by the cells with 1.0 MPa. The lithium vs. LTO cells with LP57 with 5 wt% FEC demonstrate an enhanced performance compared to those with LP57. The capacity retention is around 95.8% after 250 cycles for the cells with 1.0 MPa external bracing. The stable performance for hundreds of cycles is related to the more stable SEI on the lithium metal and the reduced formation of dead lithium.[30–36] The cells show a capacity drop shortly before reaching 80% of the initial capacity, followed by a short phase of recovery before the capacity fades again. This capacity fading-recovery-fading phenomenon is present for all applied external pressures, but is shifted to later cycles in the cells with the highest pressure. It should be noted that the standard deviation is higher for the cells with 0.5 MPa as this behavior occurs for one cell at ~200 cycles and for the other cell at ~250 cycles.

For a better understanding of this phenomenon and to check if there is an electrolyte or separator dependency, cells with a lower amount of electrolyte and a different separator were built (Figure 5). The capacity fading-recovery-fading phenomenon is present for all cells built but with some variations in terms of the cycling stage and the intensity of fading. The cells with 100 µL electrolyte show the phenomenon at an earlier stage in the cycling compared to the cells with 300 µL. For the cells with a 260 µm glass fiber separator (Whatman GF/C) and 200 µL electrolyte the initial capacity fading is mitigated but still visible. The varying cycling stage

Research Article
doi.org/10.1002/batt.202200452
Chemistry Europe
European Chemical Societies Publishing

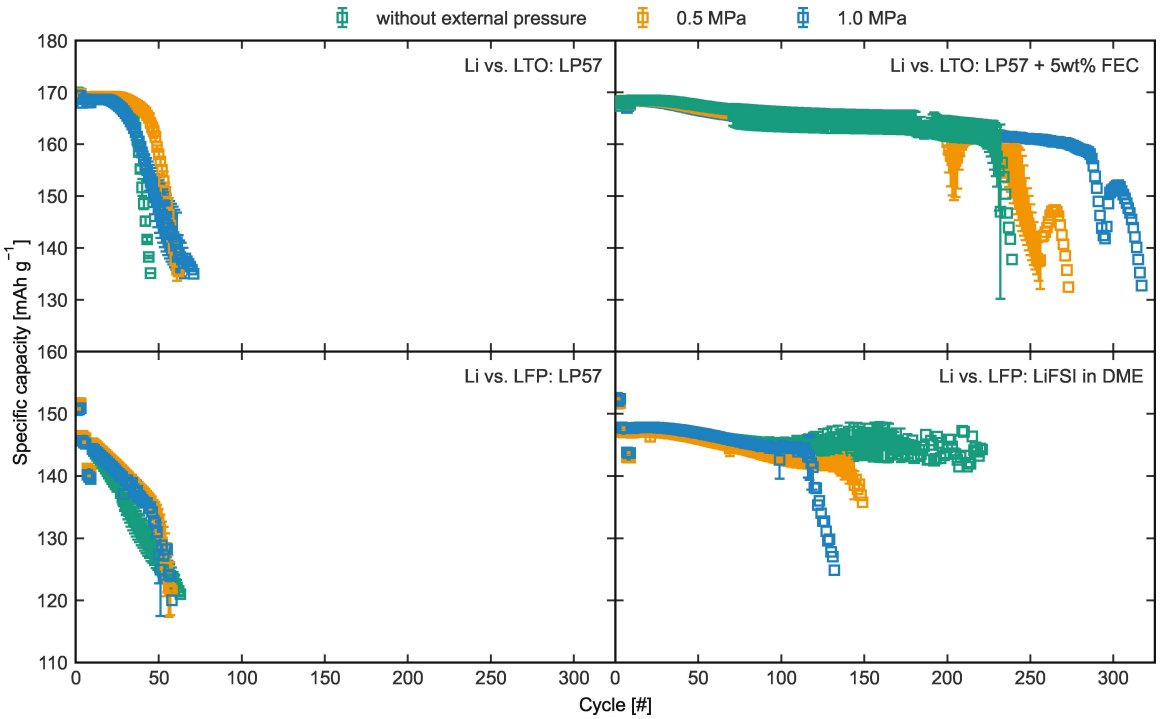

Figure 4. Specific capacity as a function of cycle for the cycling of lithium vs. LTO or LFP with different electrolytes (LP57, LP57 with 5 wt% FEC and 1 M LiFSI in DME) and various external applied pressures (without external pressure, 0.5 MPa and 1.0 MPa).

and intensity of the fading indicates that the specific amount of FEC ($mol_{FEC}/g_{electrode}$) is responsible for this phenomenon. Jung et al. showed enhanced performance of lithium vs. silicon cells containing an increased amount of FEC additive in the cells compared to cells with a lower amount of additive in the electrolyte.[32] Saltira et al. showed a capacity fading and recovery of lithium vs. NCM cells with a FEC-based electrolyte.[31] The initial capacity fading might then be related to the consumption of the FEC in the cell, which can explain the earlier appearance of the capacity fading phenomenon in the cells with the lower amount of electrolyte. The decomposition of the electrolyte when FEC is present is almost exclusively related to FEC, as it is easier to decompose compared to EC or EMC. FEC has a lowest unoccupied molecular orbital (LUMO) that is lower in energy than that of EC and EMC with values of −0.87 eV, −0.38 eV and −0.26 eV, respectively.[33,37] As a result, the SEI has an increased LiF content, which makes the SEI thick and more stable when FEC is present.[32,33,38] The capacity recovery, after the FEC has been consumed, might then be a result of SEI cracking, followed by the formation of a new, thinner SEI due to the reduction of EC/EMC. The newly-formed SEI might be initially thinner, but is more unstable for continuously cycling. As a result, the capacity recovers for some cycles before the dead lithium and the dendrite growth, likely facilitated by a less robust or stable SEI, lead to the capacity fading. Higher external pressure reduces the formation of mossy and dead lithium, and hence, also the side reactions and consumption of the electrolyte with the lithium metal. Hence, the capacity fading-recovery-fading phenomenon is shifted to a later phase during cycling.

To determine the impact of the LiFSI-based electrolyte and the effect of the counter electrode on the pressure-dependent performance of the lithium metal cells LFP was chosen as a second counter electrode. When the carbonate-based electrolyte LP57 is used, the lithium vs. LFP cells yield similar results as the LTO cells, i.e., the 80% capacity threshold is reached after around 60 cycles (Figure 4c). For around 50 cycles, the cells with higher pressure have an increased capacity retention compared to the cells without external applied pressure. Nevertheless, the cells with the high external pressure have a sudden capacity drop after ~50 cycles, whereas the cells without external pressure do not show this sudden capacity fading behavior.

The lithium vs. LFP cells with 1 M LiFSI in DME show stable cycling up to around 100 cycles, but there is no evidence of a dependance on pressure in this experiment (Figure 4d). The capacity retention after 100 cycles is ~98%. This proves that a relatively stable SEI is present on the lithium metal with the ether-based electrolyte, which limits the formation of dead lithium.[9,39] After around 100 cycles, the capacity of the individual cells starts to scatter, which is probably related to drying due to consumption of the electrolyte. The consumption of the electrolyte, which in this case leads to gassing (Figure S5), is a significant degradation mechanism, which makes it difficult to cycle the cells longer than ~100 cycles. Overall, the results in this section show that while the influence of the counter electrode on the performance of the lithium metal cells is small, whereas the choice of electrolyte and external pressure play a more dominant role.

Research Article
doi.org/10.1002/batt.202200452
Chemistry Europe
European Chemical Societies Publishing

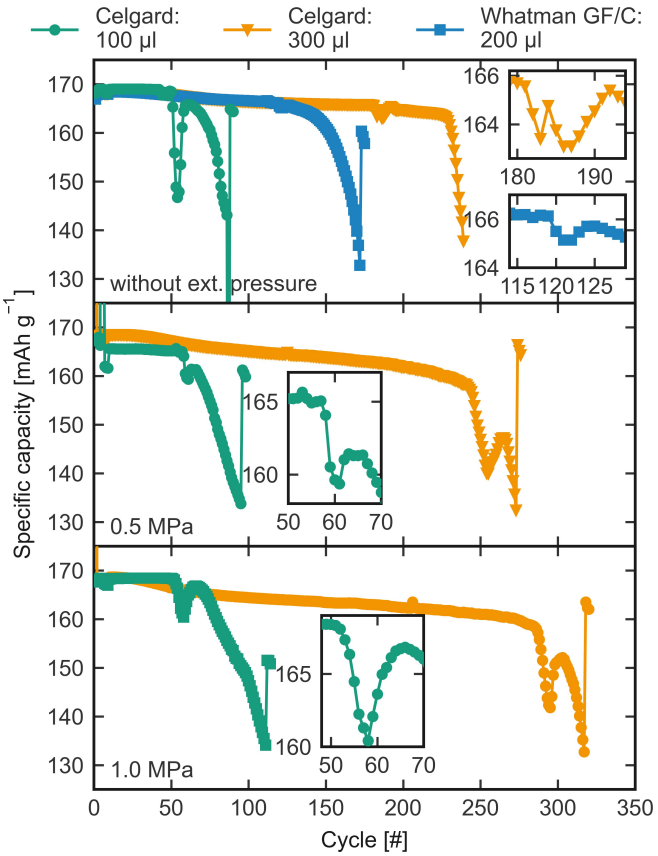

Figure 5. Capacity fading-recovery-fading phenomenon of representative lithium vs. LTO cells with different amounts of electrolyte, different separators and different applied external pressures. For better visibility, only one representative cell is shown for each parameter.

Figure 6 shows the pressure evolution of the cells with an external applied pressure over the time. Regardless of the applied pressure or electrolyte used, the pressure increases for all cells over cycling. Nevertheless, the cells with an initial applied pressure of 0.5 MPa show a more significant increase of the pressure compared to the cells with 1.0 MPa, e.g., by a factor of at least 2, which can be related to the more significant increase of the irreversible expansion of the lithium metal (Figure 3). This is further evidence for the reduced formation of mossy and dead lithium in cells with a high applied external pressure.

The pressure increase is also influenced by the type of electrolyte. The use of the LP57 (carbonate-based electrolyte without an additive) results in a tremendous increase of the pressure during cycling at high current densities ($>1.0\ mA\,cm^{-2}$). The cells with the FEC additive still have a significant increase of the pressure, but this increase is less pronounced than the cells without additive. After 1000 h of cycling the pressure on the electrodes increased from 0.5 MPa and 1.0 MPa up to only ~0.8 MPa and ~1.1 MPa, respectively. Subsequently, a significant pressure change is visible after ~1100 h (0.5 MPa) and ~1580 h (1.0 MPa). At this point (Cycle 204 at 0.5 MPa and cycle 295 at 1.0 MPa), the capacity starts to recover from the initial capacity fading (Figures 4 and 5) as part of the capacity fading-recovery-fading phenomenon. This behavior is further evidence that at this point the FEC has been consumed and that reduction of the EC/EMC has started. Combined with the results above, this shows the beneficial impact of the FEC on a stable SEI, which suppresses the formation of dead lithium. The cells with ether-based electrolyte undergo the highest pressure increase over the cycling. However, this result is probably a combination of several effects and gassing likely plays the most significant role (Figure S5).

Conclusion

The cycling of lithium metal half cells in an *operando* dilation cell and in laboratory-scale pouch cells reveal the beneficial effect of external pressure on the cycling performance. The thickness of lithium stripped and plated is much higher than theoretically expected at low applied external pressures. The difference comes from SEI formation and the deposition morphology that is not homogeneous which leads to formation of mossy and dead lithium. The irreversible expansion of lithium is significantly reduced with increasing external pressure on the cells. The smaller irreversible expansion is most likely related to the reduced formation of mossy and dead lithium at higher pressures due to enhanced electrical contact between the bulk and mossy lithium.

Another significant factor in the performance of the lithium metal half cells is the choice of the electrolyte. Standard carbonate-based electrolytes show a high pressure or irreversible dilation increase and poor performance. The addition of an additive like FEC or the use of ether-based electrolytes can significantly reduce the pressure or irreversible expansion increase over the cycling, which is mostly related to a stable SEI. Furthermore, the specific amount of the FEC additive in the carbonate-based electrolyte is an important aspect. The cells with a larger amount of FEC performed significantly better than those with a smaller amount of FEC. The continuous formation of SEI on fresh lithium during stripping and plating leads to the consumption of the FEC. When all the FEC has been consumed, the capacity of the cell fades due to the poorer stability of the newly-formed SEI resulting from the reduction of the other carbonates in the electrolyte.

Overall, this work shows the importance of pressure and electrolyte choice for lithium metal cells. This result is not only important for future battery systems, but also for SoA battery research. When testing electrodes in half-cells, the limitation of the lithium metal should also be considered, especially at high current rates and when a low external pressure is applied. The addition of a sufficient amount of FEC to standard carbonate electrolytes can also help to reduce the impact of lithium metal on the performance of electrodes in half-cells.

Research Article
doi.org/10.1002/batt.202200452
Chemistry Europe
European Chemical Societies Publishing

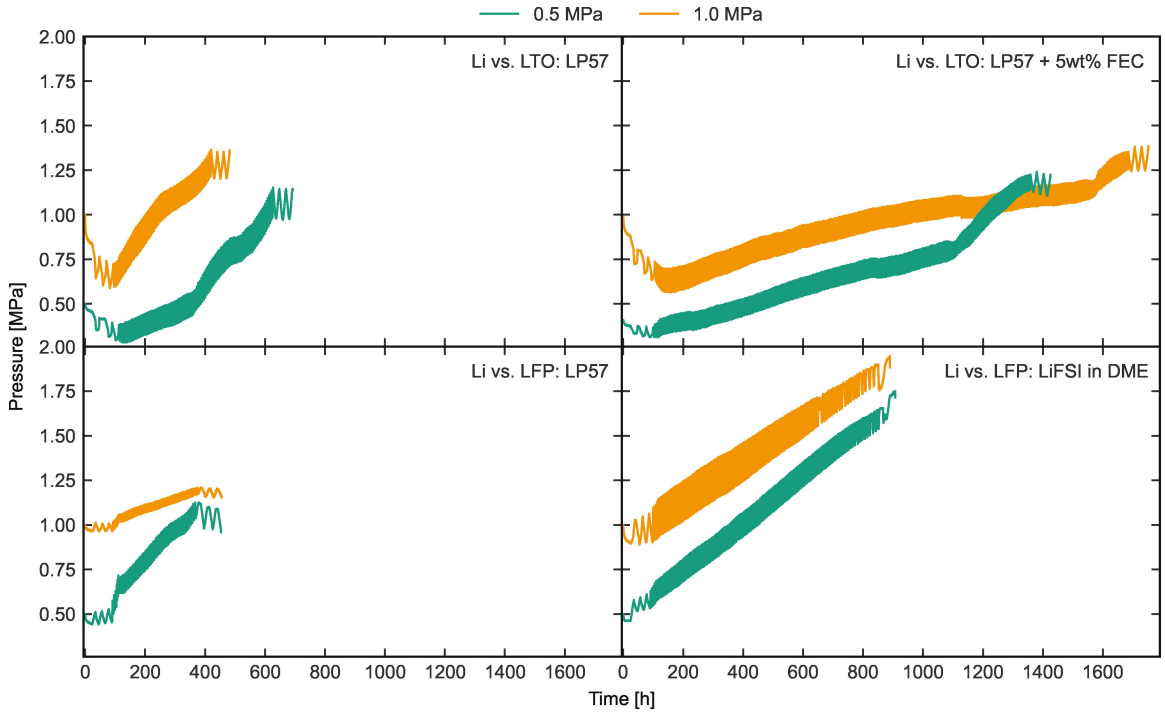

Figure 6. Pressure as a function of time for the cells with 0.5 MPa and 1.0 MPa initially applied external pressure. For better visibility, only one representative cell is shown for each parameter.

Experimental Section

Materials

Lithium metal, $Li_4Ti_5O_{12}$ (LTO), $LiFePO_4$ (LFP), graphite, $LiNi_{0.33}Co_{0.33}Mn_{0.33}O_2$ (NCM111) and silicon were used as electrodes (Table 2). The loading of the electrodes were between 2.0 and 2.2 mAh cm^{-2} for the commercial electrodes and ~2.5 mAh cm^{-2} for the silicon electrodes fabricated in house. It should be noted that the actual capacity utilized is around 72% for the silicon electrodes. Before using lithium as an anode material, the surface was cleaned by scraping off the passivation layer with a ceramic knife and then flattened with a roll to obtain a flat and smooth surface. Before the cycling experiments, the electrodes were punched into 18 mm discs (silicon: 16 mm) and then dried in a glovebox oven at 120 °C for 12 hours under vacuum. The lithium metal was punched into 18 mm discs for the dilation cell and to approx. 20×20 mm pieces for the pouch cells. CG2500 (Celgard LLC) with a thickness of 25 µm and porosity of 55% was used as separator in all experiments, unless otherwise noted. The separator was dried in a glovebox oven at 50 °C for 12 hours under vacuum. Three different types of electrolytes were used in this work: (1) 1 M $LiPF_6$ in ethylene carbonate (EC)/ethyl methyl carbonate (EMC) 3/7 wt% (LP57, Gotion Inc.), (2) LP57 with 5 wt% fluoroethylene carbonate (FEC, BASF SE) and (3) the ether-based 1 M LiFSI (Arkema) in DME (Merck KGaA).

Table 2. Properties (i.e., areal loading, thickness of the active material, porosity and distributor) of the electrodes used in this study.

Electrode	Areal loading [mAh cm^{-2}]	Thickness [µm]	Porosity [%]	Distributor
Lithium	–	380	–	Merck KGaA
LTO	2.0	115	64	Customcells Holding GmbH
LFP	2.0	88	51	Customcells Holding GmbH
Graphite	2.2	71	35	Customcells Holding GmbH
NCM111	2.0	100	40	Customcells Holding GmbH
Silicon	~2.5	~18	~75	Self-fabricated[40]

Dilation cell and bracing cell

The expansion behavior of the electrodes was measured in a dilatometry setup.[41] In this setup, the expansion of an electrode stack was measured under various applied mechanical forces. For more detailed information about the dilation cell, the reader is referred to the following Ref. [41]. The electrode stack consists of two 18 mm electrodes and a 21.6 mm separator. The applied external mechanical pressures were 0.05 MPa, 0.5 MPa and 1.0 MPa. The amount of electrolyte was 200 µL.

To investigate the impact of the external applied pressure on the cell performance, laboratory pouch cells were built with lithium metal as the working electrolyte, LTO or LFP as counter electrodes and CG2500 (approx. 33×33 mm) as separator. Two 20 mm stainless steel spacers (placed between the electrode and the current collector tab) were used to homogenize the pressure distribution on the electrode stack. The amount of electrolyte was 100 µL for the cells with LP57 and 300 µL for the cells with LP57 with 5 wt% FEC and 1 M LiFSI in DME. The higher electrolyte amount for the LP57 with 5 wt% FEC and 1 M LiFSI in DME was used to prevent rapid drying out of the electrolyte in the cell. The pouch cells were placed in a self-built bracing device, where an aluminum plate presses against the cell and a load cell measures the pressure.[40] The external applied pressures were 0.5 MPa and 1.0 MPa. Furthermore, pouch cells without external pressure were cycled. The internal pressure from the vacuum sealing of the pouch cells is in the range of 0.05–0.1 MPa and hence comparable to the

performance with the cells in the dilation cell with an external pressure of 0.05 MPa.

Electrochemical measurements

The experiments with the dilation cell were conducted inside an argon-filled glovebox (O_2 and H_2O < 1 ppm, M. BRAUN Inertgas-Systeme GmbH) to avoid the infiltration of air into the cell. The electrochemical tests were performed with a ModuLab XM MTS System (Solartron Analytical), where the applied pressure and the dilation were recorded along with the full cell voltage. For the initial investigation of the electrode expansion and the selection of the counter electrode for subsequent testing, different electrode combinations were cycled (graphite vs. NCM111, NCM111 vs. LTO, LFP vs. LTO, Li vs. LTO, graphite vs. LTO and Si vs. NCM111). The applied pressure was 0.05 MPa, CG 2500 was used as separator and LP57 and LP57 + FEC (silicon vs. LTO) were used as the electrolyte. The current was 2.0 mA cm^{-2}. During the irreversible dilation measurements of lithium vs. LTO or LFP, all cells were cycled with three initial 0.1 C (0.2 mA cm^{-2}) formation cycles, followed by three 0.5 C (1.0 mA cm^{-2}) cycles, 30 1.0 C (2.0 mA cm^{-2}) cycles and again three 0.5 C (1.0 mA cm^{-2}) cycles. The C-rate was related to the nominal capacity of the counter electrodes, which was 5.09 mAh (i.e., 2.0 mAh cm^{-2} × 2.545 cm^2). The temperature was set to 25 °C and controlled with a self-built temperature device during the measurement. The lithiation of the LTO and the delithiation of the LFP ('discharging' for LTO - and 'charging' for LFP system) was conducted in a constant current constant voltage (CCCV) mode, with a cut-off criterion during the CV step of I < 0.04 C for 0.1 C and 0.5 C and I < 0.1 C for 1.0 C, respectively, at the cutoff voltage. The Li vs. LTO cells were cycled between 1.3 V and 2.0 V and the Li vs. LFP cells were cycled between 2.5 V and 3.8 V. All cell combinations were built at least twice.

The electrochemical tests for the pouch cells were performed with a Maccor Series 4000 battery tester (Maccor Inc.) in a climate chamber at 25 °C. The cells (i.e., Li vs. LTO/LFP) were cycled with three initial 0.1 C (0.2 mA cm^{-2}) formation cycles, followed by three 0.5 C (1.0 mA cm^{-2}) cycles, three 1.0 C (2.0 mA cm^{-2}) cycles and then cycled with 0.5 C (1.0 mA cm^{-2}) until 80 % of the initial 0.1 C capacity is reached. The lithiation of the LTO and the delithiation of the LFP was also conducted with CCCV procedure, with a voltage cutoff of 1.3 V and 3.8 V, respectively, and a cutoff of 10 % of the applied current (e.g., I < 0.1 C for 1.0 C). All cells with standard deviation shown were obtained from at least two separate cells.

Acknowledgements

The authors gratefully acknowledge the funding of this work by the Federal Ministry for Economic Affairs and Climate Action (BMWK) of Germany in the project ReViSEDBatt (grant number 03ETE004 A) and the Bavarian Ministry of Economic Affairs and Media, Energy and Technology for funding the Fraunhofer R&D Center for Electromobility Bavaria FZEB (Grant number: 43-6629/86). We also want to thank Prof. Dr. Gerhard Sextl and the members of the Fraunhofer R&D Center Electromobility at Fraunhofer ISC for fruitful discussions, scientific support, proof-reading and especially the technical support of Ajana Gebel, Vilija Anfimovaite, Franziska Stahl. Open Access funding enabled and organized by Projekt DEAL.

Conflict of Interest

The authors declare no conflict of interest.

Data Availability Statement

The data that support the findings of this study are available from the corresponding author upon reasonable request.

Keywords: electrochemistry · dead lithium · dilation · lithium · lithium metal cell · pressure

[1] M. Winter, B. Barnett, K. Xu, *Chem. Rev.* **2018**, *118*, 11433.
[2] D. Lin, Y. Liu, Y. Cui, *Nat. Nanotechnol.* **2017**, *12*, 194.
[3] C. Fang, X. Wang, Y. S. Meng, *Trends Chem.* **2019**, *1*, 152.
[4] X.-B. Cheng, R. Zhang, C.-Z. Zhao, Q. Zhang, *Chem. Rev.* **2017**, *117*, 10403.
[5] W. Xu, J. Wang, F. Ding, X. Chen, E. Nasybulin, Y. Zhang, J.-G. Zhang, *Energy Environ. Sci.* **2014**, *7*, 513.
[6] G. A. Giffin, *Nat. Commun.* **2022**, *13*, 5250.
[7] X. Gao, Y.-N. Zhou, D. Han, J. Zhou, D. Zhou, W. Tang, J. B. Goodenough, *Joule* **2020**, *4*, 1864.
[8] K. N. Wood, M. Noked, N. P. Dasgupta, *ACS Energy Lett.* **2017**, *2*, 664.
[9] Y. Xu, K. Dong, Y. Jie, P. Adelhelm, Y. Chen, L. Xu, P. Yu, J. Kim, Z. Kochovski, Z. Yu, W. Li, J. LeBeau, Y. Shao-Horn, R. Cao, S. Jiao, T. Cheng, I. Manke, Y. Lu, *Adv. Energy Mater.* **2022**, *12*, 2200398.
[10] J. Steiger, G. Richter, M. Wenk, D. Kramer, R. Mönig, *Electrochem. Commun.* **2015**, *50*, 11.
[11] P. Daubinger, M. Schelter, R. Petersohn, F. Nagler, S. Hartmann, M. Herrmann, G. A. Giffin, *Adv. Energy Mater.* **2021**, *12*, 2102448.
[12] M. Wünsch, J. Kaufman, D. U. Sauer, *J. Energy Storage* **2019**, *21*, 149.
[13] F. Ebert, G. Sextl, M. Lienkamp **2017**, http://ieeexplore.ieee.org/servlet/opac?punumber=7933062.
[14] J. Cannarella, C. B. Arnold, *J. Power Sources* **2014**, *245*, 745.
[15] L. Qin, K. Wang, H. Xu, M. Zhou, G. Yu, C. Liu, Z. Sun, J. Chen, *Nano Energy* **2020**, *77*, 105098.
[16] C. Niu, H. Lee, S. Chen, Q. Li, J. Du, W. Xu, J.-G. Zhang, M. S. Whittingham, J. Xiao, J. Liu, *Nat. Energy* **2019**, *4*, 551.
[17] X. Zhang, Q. J. Wang, K. L. Harrison, K. Jungjohann, B. L. Boyce, S. A. Roberts, P. M. Attia, S. J. Harris, *J. Electrochem. Soc.* **2019**, *166*, A3639-A3652.
[18] X. Yin, W. Tang, D. Im Jung, K. C. Phua, S. Adams, S. W. Lee, G. W. Zheng, *Nano Energy* **2018**, *50*, 659.
[19] M. Ue, K. Uosaki, *Curr. Opinion Electrochem.* **2019**, *17*, 106.
[20] Y. Li, Z. Yang, Z. Wu, J. Li, J. Zou, C. Jiang, J. Yang, L. Wang, X. Niu, *Proc. Symposium on Materials for Advanced Batteries and Fuel Cells* **2018**, *324*, 144.
[21] J. Qian, W. A. Henderson, W. Xu, P. Bhattacharya, M. Engelhard, O. Borodin, J.-G. Zhang, *Nat. Commun.* **2015**, *6*, 6362.
[22] H. Yan, D. Zhang, Qilu, X. Duo, X. Sheng, *Ceram. Intern.* **2021**, *47*, 5870.
[23] L. de Biasi, A. O. Kondrakov, H. Geßwein, T. Brezesinski, P. Hartmann, J. Janek, *J. Phys. Chem. C* **2017**, *121*, 26163.
[24] D. Sauerteig, S. Ivanov, H. Reinshagen, A. Bund, *J. Power Sources* **2017**, *342*, 939.
[25] M. Nagayama, K. Ariyoshi, Y. Yamamoto, T. Ohzuku, *J. Electrochem. Soc.* **2014**, *161*, A1388-A1393.
[26] M. N. Obrovac, V. L. Chevrier, *Chem. Rev.* **2014**, *114*, 11444.
[27] K. Feng, M. Li, W. Liu, A. G. Kashkooli, X. Xiao, M. Cai, Z. Chen, *Small* **2018**, *14*, 1702737.
[28] T. R. Jow, K. Xu, O. Borodin, M. Ue, *Electrolytes for Lithium and Lithium-Ion Batteries*, Springer New York, New York, NY **2014**.
[29] K. Xu, *Chemical reviews* **2014**, *114*, 11503.
[30] P. Zhai, L. Liu, X. Gu, T. Wang, Y. Gong, *Adv. Energy Mater.* **2020**, *10*, 2001257.
[31] G. Salitra, E. Markevich, M. Afri, Y. Talyosef, P. Hartmann, J. Kulisch, Y.-K. Sun, D. Aurbach, *ACS Appl. Mater. Interfaces* **2018**, *10*, 19773.

Research Article
doi.org/10.1002/batt.202200452

[32] R. Jung, M. Metzger, D. Haering, S. Solchenbach, C. Marino, N. Tsiouvaras, C. Stinner, H. A. Gasteiger, *J. Electrochem. Soc.* **2016**, *163*, A1705-A1716.
[33] X.-Q. Zhang, X.-B. Cheng, X. Chen, C. Yan, Q. Zhang, *Adv. Funct. Mater.* **2017**, *27*, 1605989.
[34] R. Petibon, V. L. Chevrier, C. P. Aiken, D. S. Hall, S. R. Hyatt, R. Shunmugasundaram, J. R. Dahn, *J. Electrochem. Soc.* **2016**, *163*, A1146-A1156.
[35] H. Shin, J. Park, A. M. Sastry, W. Lu, *J. Electrochem. Soc.* **2015**, *162*, A1683-A1692.
[36] K. Schroder, J. Alvarado, T. A. Yersak, J. Li, N. Dudney, L. J. Webb, Y. S. Meng, K. J. Stevenson, *Chem. Mater.* **2015**, *27*, 5531.
[37] X. Shen, P. Li, X. Liu, S. Chen, X. Ai, H. Yang, Y. Cao, *Chem. Sci.* **2021**, *12*, 9037.
[38] Z.-C. Wang, J. Xu, W.-H. Yao, Y.-W. Yao, Y. Yang, *ECS Trans.* **2012**, *41*, 29.
[39] H. Wu, H. Jia, C. Wang, J.-G. Zhang, W. Xu, *Adv. Energy Mater.* **2021**, *11*, 2003092.
[40] M. Göttlinger, P. Daubinger, W. Stracke, S. Hartmann, G. A. Giffin, *Electrochim. Acta* **2022**, *419*, 140354.
[41] P. Daubinger, F. Ebert, S. Hartmann, G. A. Giffin, *J. Power Sources* **2021**, *488*, 229457.

Manuscript received: October 14, 2022
Revised manuscript received: November 18, 2022
Version of record online: December 16, 2022